Hard Exclusive Electroproduction of $\pi^+\pi^-$ Pairs

A. Airapetian,[18] N. Akopov,[31] Z. Akopov,[31] M. Amarian,[8,31] V.V. Ammosov,[23] A. Andrus,[16] E.C. Aschenauer,[8] W. Augustyniak,[30] R. Avakian,[31] A. Avetissian,[31] E. Avetissian,[12] P. Bailey,[16] D. Balin,[22] V. Baturin,[22] M. Beckmann,[7] S. Belostotski,[22] S. Bernreuther,[10] N. Bianchi,[12] H.P. Blok,[21,29] H. Böttcher,[8] A. Borissov,[15] A. Borysenko,[12] M. Bouwhuis,[16] J. Brack,[6] A. Brüll,[17] V. Bryzgalov,[23] G.P. Capitani,[12] T. Chen,[4] G. Ciullo,[11] M. Contalbrigo,[11] P.F. Dalpiaz,[11] R. De Leo,[3] M. Demey,[21] L. De Nardo,[1] E. De Sanctis,[12] E. Devitsin,[19] P. Di Nezza,[12] M. Düren,[14] M. Ehrenfried,[10] A. Elalaoui-Moulay,[2] G. Elbakian,[31] F. Ellinghaus,[8] U. Elschenbroich,[13] R. Fabbri,[11] A. Fantoni,[12] A. Fechtchenko,[9] L. Felawka,[27] S. Frullani,[25] G. Gapienko,[23] V. Gapienko,[23] F. Garibaldi,[25] K. Garrow,[1,26] E. Garutti,[21] G. Gavrilov,[7,27] V. Gharibyan,[31] G. Graw,[20] O. Grebeniouk,[22] L.G. Greeniaus,[1,27] I.M. Gregor,[8] K.A.Griffioen,[21,32] K. Hafidi,[2] M. Hartig,[27] D. Hasch,[12] D. Heesbeen,[21] M. Henoch,[10] R. Hertenberger,[20] W.H.A. Hesselink,[21,29] A. Hillenbrand,[10] M. Hoek,[14] Y. Holler,[7] B. Hommez,[13] G. Iarygin,[9] A. Ivanilov,[23] A. Izotov,[22] H.E. Jackson,[2] A. Jgoun,[22] R. Kaiser,[15] E. Kinney,[6] A. Kisselev,[6] M. Kopytin,[8] V. Korotkov,[23] V. Kozlov,[19] B. Krauss,[10] V.G. Krivokhijine,[9] L. Lagamba,[3] L. Lapikás,[21] A. Laziev,[21,29] P. Lenisa,[11] P. Liebing,[8] L.A. Linden-Levy,[16] K. Lipka,[8] W. Lorenzon,[18] H. Lu,[5] J. Lu,[27] S. Lu,[14] B.-Q. Ma,[4] B. Maiheu,[13] N.C.R. Makins,[16] Y. Mao,[4] B. Marianski,[30] H. Marukyan,[31] F. Masoli,[11] V. Mexner,[21] N. Meyners,[7] O. Mikloukho,[22] C.A. Miller,[1,27] Y. Miyachi,[28] V. Muccifora,[12] A. Nagaitsev,[9] E. Nappi,[3] Y. Naryshkin,[22] A. Nass,[10] M. Negodaev,[8] W.-D. Nowak,[8] K. Oganessyan,[7,12] H. Ohsuga,[28] A. Osborne,[15] N. Pickert,[10] S. Potashov,[19] D.H. Potterveld,[2] M. Raithel,[10] D. Reggiani,[11] P.E. Reimer,[2] A. Reischl,[21] A.R. Reolon,[12] C. Riedl,[10] K. Rith,[10] G. Rosner,[15] A. Rostomyan,[31] L. Rubacek,[14] J. Rubin,[16] D. Ryckbosch,[13] Y. Salomatin,[23] I. Sanjiev,[2,22] I. Savin,[9] A. Schäfer,[24] C. Schill,[12] G. Schnell,[8] K.P. Schüler,[7] J. Seele,[16] R. Seidl,[10] B. Seitz,[14] R. Shanidze,[10] C. Shearer,[15] T.-A. Shibata,[28] V. Shutov,[9] K. Sinram,[7] W. Sommer,[14] M. Stancari,[11] M. Statera,[11] E. Steffens,[10] J.J.M. Steijger,[21] H. Stenzel,[14] J. Stewart,[8] F. Stinzing,[10] P. Tait,[10] H. Tanaka,[28] S. Taroian,[31] B. Tchuiko,[23] A. Terkulov,[19] A. Tkabladze,[13] A. Trzcinski,[30] M. Tytgat,[13] A. Vandenbroucke,[13] P. van der Nat,[21] G. van der Steenhoven,[21] Y. van Haarlem,[13] M.C. Vetterli,[26,27] V. Vikhrov,[22] M.G. Vincter,[1] C. Vogel,[10] M. Vogt,[10] J. Volmer,[8] C. Weiskopf,[10] J. Wendland,[26,27] J. Wilbert,[10] G. Ybeles Smit,[29] Y. Ye,[5] Z. Ye,[5] S. Yen,[27] B. Zihlmann,[21] and P. Zupranski[30]

(The HERMES Collaboration)

Submitted to Physics Letters B

[1] *Department of Physics, University of Alberta, Edmonton, Alberta T6G 2J1, Canada*
[2] *Physics Division, Argonne National Laboratory, Argonne, Illinois 60439-4843, USA*
[3] *Istituto Nazionale di Fisica Nucleare, Sezione di Bari, 70124 Bari, Italy*
[4] *School of Physics, Peking University, Beijing 100871, China*
[5] *Department of Modern Physics, University of Science and Technology of China, Hefei, Anhui 230026, China*
[6] *Nuclear Physics Laboratory, University of Colorado, Boulder, Colorado 80309-0446, USA*
[7] *DESY, Deutsches Elektronen-Synchrotron, 22603 Hamburg, Germany*
[8] *DESY Zeuthen, 15738 Zeuthen, Germany*
[9] *Joint Institute for Nuclear Research, 141980 Dubna, Russia*
[10] *Physikalisches Institut, Universität Erlangen-Nürnberg, 91058 Erlangen, Germany*
[11] *Istituto Nazionale di Fisica Nucleare, Sezione di Ferrara and Dipartimento di Fisica, Università di Ferrara, 44100 Ferrara, Italy*
[12] *Istituto Nazionale di Fisica Nucleare, Laboratori Nazionali di Frascati, 00044 Frascati, Italy*
[13] *Department of Subatomic and Radiation Physics, University of Gent, 9000 Gent, Belgium*
[14] *Physikalisches Institut, Universität Gießen, 35392 Gießen, Germany*
[15] *Department of Physics and Astronomy, University of Glasgow, Glasgow G12 8QQ, United Kingdom*
[16] *Department of Physics, University of Illinois, Urbana, Illinois 61801-3080, USA*
[17] *Laboratory for Nuclear Science, Massachusetts Institute of Technology, Cambridge, Massachusetts 02139, USA*
[18] *Randall Laboratory of Physics, University of Michigan, Ann Arbor, Michigan 48109-1120, USA*
[19] *Lebedev Physical Institute, 117924 Moscow, Russia*
[20] *Sektion Physik, Universität München, 85748 Garching, Germany*
[21] *Nationaal Instituut voor Kernfysica en Hoge-Energiefysica (NIKHEF), 1009 DB Amsterdam, The Netherlands*
[22] *Petersburg Nuclear Physics Institute, St. Petersburg, Gatchina, 188350 Russia*
[23] *Institute for High Energy Physics, Protvino, Moscow region, 142281 Russia*
[24] *Institut für Theoretische Physik, Universität Regensburg, 93040 Regensburg, Germany*

[25]Istituto Nazionale di Fisica Nucleare, Sezione Roma 1, Gruppo Sanità and Physics Laboratory, Istituto Superiore di Sanità, 00161 Roma, Italy
[26]Department of Physics, Simon Fraser University, Burnaby, British Columbia V5A 1S6, Canada
[27]TRIUMF, Vancouver, British Columbia V6T 2A3, Canada
[28]Department of Physics, Tokyo Institute of Technology, Tokyo 152, Japan
[29]Department of Physics and Astronomy, Vrije Universiteit, 1081 HV Amsterdam, The Netherlands
[30]Andrzej Soltan Institute for Nuclear Studies, 00-689 Warsaw, Poland
[31]Yerevan Physics Institute, 375036 Yerevan, Armenia
[32]Permanent Address: College of William & Mary, Williamsburg, VA 23187

Hard exclusive electroproduction of $\pi^+\pi^-$ pairs off hydrogen and deuterium targets has been studied by the HERMES experiment at DESY. Legendre moments $\langle P_1\rangle$ and $\langle P_3\rangle$ of the angular distributions of π^+ mesons in the center-of-mass frame of the pair have been measured for the first time. Their dependence on the $\pi^+\pi^-$ invariant mass can be understood as being due to the interference between relative P-wave (isovector) and S, D-wave (isoscalar) states of the two pions. The increase in magnitude of $\langle P_1\rangle$ as Bjorken x increases is interpreted in the framework of Generalized Parton Distributions as an enhancement of flavour non-singlet $q\bar{q}$ exchange for larger values of x, which leads to a sizable admixture of isoscalar and isovector pion pairs. In addition, the interference between P-wave and D-wave states separately for transverse and longitudinal pion pairs has been studied. The data indicate that in the $f_2(1270)$ region at $\langle Q^2\rangle = 3$ GeV^2 higher-twist effects can be as large as the leading-twist longitudinal component.

PACS numbers: 13.60.Le, 14.40.Cs, 25.30.Rw, 13.88.+e

Much of our current knowledge of the quark-gluon structure of the nucleon comes from inclusive and semi-inclusive deep inelastic scattering experiments, from which parton distribution functions can be extracted. However, our understanding of quark-gluon dynamics can be extended considerably by measurements sensitive to the generalized parton distributions (GPD) [1–3], which also describe the dynamical correlations between partons with different momenta. Experimentally, GPDs can be investigated through the analysis of hard exclusive processes such as the production of mesons by longitudinal virtual photons. Under these conditions the amplitude factorizes into a hard scattering term governed by perturbative QCD and two soft parts, the GPDs for the nucleon and the distribution amplitude for meson formation [4, 5]. Hard exclusive electroproduction of $\pi^+\pi^-$ pairs is sensitive to the interference between isospin $I = 1$ and $I = 0$ channels, and provides a new constraint on certain combinations of GPDs.

This letter reports the first experimental data for hard exclusive $\pi^+\pi^-$ pair production

$$e^+p \to e^+p\,\pi^+\pi^- \quad \text{and} \quad e^+d \to e^+d\,\pi^+\pi^- \ . \qquad (1)$$

For the proton target, the results are interpreted in the GPD framework by comparing with predictions [6–8], thus providing valuable information for further modelling of GPDs. So far, predictions exist only for the proton target. Exclusive pair production includes contributions from both two-gluon and quark-antiquark ($q\bar{q}$) exchange mechanisms.

The relevant diagrams at leading twist, which may involve both resonant and non-resonant channels, are shown in Fig. 1. The Primakoff process $\gamma^\star\gamma^\star \to \pi^+\pi^-$ is not shown, because it is expected to contribute negligibly to the production of pions pairs with helicity zero or one [9], and the analysis reported here is insensitive to helicity two. Previous work [10] has shown that resonant $\pi^+\pi^-$ production via longitudinal ρ^0 decay in the kinematical region covered by the HERMES experiment occurs primarily through two-quark exchange with the target. In the present more general case, the $q\bar{q}$ exchange mechanism gives rise to pion pairs with the values of the strong isospin I, total angular momentum J, and C-parity of either a ρ-meson ($I = 1$, $J = 1, 3..., C = -1$), or an f-meson ($I = 0$, $J = 0, 2..., C = +1$). The $q\bar{q}$ exchange with $C = +1$ ($C = -1$) is described by flavour singlet (non-singlet) parton combinations [11], and due to C-parity conservation the $\pi^+\pi^-$ pairs so formed have $C = -1$ ($C = +1$). The competing two-gluon channel gives rise to pion pairs with the quantum numbers of the ρ-meson family only. Pion pairs are formed from either quarks (Fig. 1-a,b,c) or gluons (Fig. 1-d) produced in the perturbative hard part of the reaction. Since the cross section for isovector $\pi^+\pi^-$ production is much larger than for the isoscalar case, it is difficult to obtain experimental data on the isoscalar channel. One possible solution would be to study exclusive $\pi^0\pi^0$ production, but this requires a large experimental acceptance. With charged pions, the interference between the two isospin channels can also provide information on the weaker isoscalar channel at the amplitude level.

For the purpose of studying the interference between $\pi^+\pi^-$ production in P-wave ($I = 1$) and S, D-wave states ($I = 0$), the Legendre moments $\langle P_1(\cos\theta)\rangle$ and $\langle P_3(\cos\theta)\rangle$ are particularly useful because they are sensitive only to such interference. The Legendre moment of order n is given by

$$\langle P_n(\cos\theta)\rangle^{\pi^+\pi^-} = \frac{\int_{-1}^{1} d\cos\theta\, P_n(\cos\theta)\, \frac{d\sigma^{\pi^+\pi^-}}{d\cos\theta}}{\int_{-1}^{1} d\cos\theta\, \frac{d\sigma^{\pi^+\pi^-}}{d\cos\theta}} \ , \qquad (2)$$

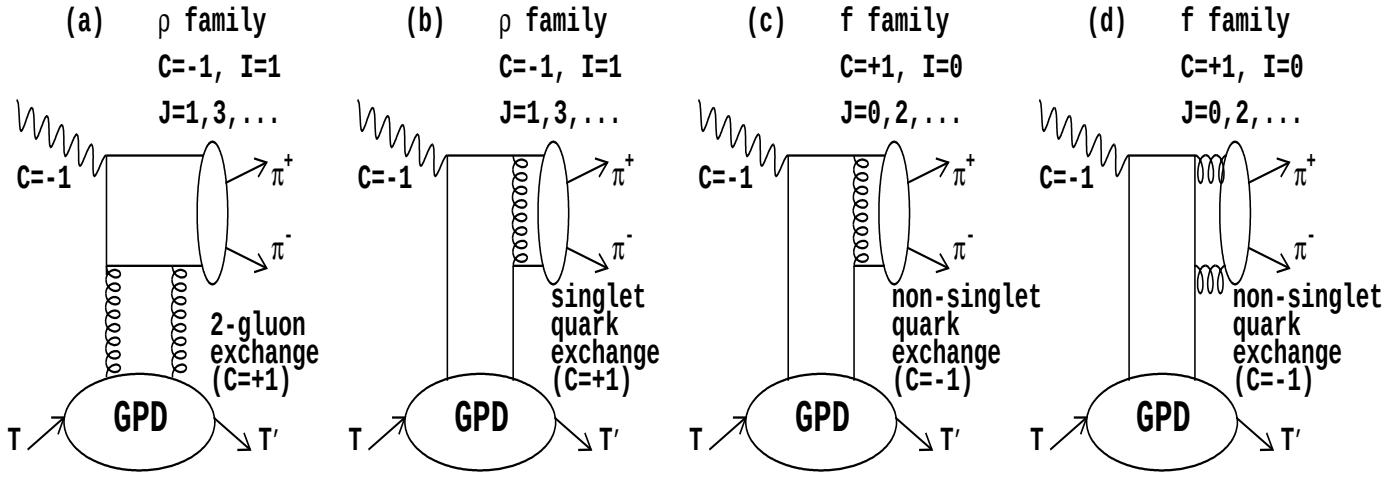

FIG. 1: Leading twist diagrams for the hard exclusive reaction $e^+T \to e^+T'\,\pi^+\pi^-$. Gluon exchange (*a)* gives rise to pions in the isovector state only, while the quark exchange mechanism (*b,c,d*) gives rise to pions in both isoscalar and isovector states.

where θ is the polar angle of the π^+ meson with respect to the direction of the $\pi^+\pi^-$ pair in the center-of-momentum frame of the virtual photon and target nucleon. The moments $\langle P_1\rangle$ and $\langle P_3\rangle$ have been evaluated as a function of the pion pair invariant mass $m_{\pi\pi}$, and the Bjorken variable $x = \frac{Q^2}{2\nu M_P}$, where $-Q^2$ is the squared four-momentum of the initial virtual photon, M_P is the proton mass and ν is the virtual photon energy in the target rest frame. Experimentally, $\langle P_n\rangle$ is the average of $P_n(\cos\theta_i)$ for all events i grouped in bins of $m_{\pi\pi}$ or x.

In general,

$$\frac{d\sigma^{\pi^+\pi^-}}{d\cos\theta} \propto \sum_{JJ'\lambda\lambda'} \rho^{JJ'}_{\lambda\lambda'} Y_{J\lambda}(\theta,\phi) Y^{\star}_{J'\lambda'}(\theta,\phi) \qquad (3)$$

in which ρ is the spin density matrix of the pion pair, whose diagonal entries $\rho^{JJ}_{\lambda\lambda}$ give the probability of producing it with angular momentum J and longitudinal projection λ, and whose off-diagonal terms describe the corresponding interference terms. If parity is conserved $\rho^{JJ'}_{\lambda\lambda'}$ is real and $\rho^{JJ'}_{\lambda\lambda'} = (-1)^{\lambda-\lambda'}\rho^{JJ'}_{-\lambda-\lambda'}$ [12]. The contributions for $J > 2$ are expected to be negligible in the $m_{\pi\pi}$-range covered by HERMES. The Legendre moments then are

$$\langle P_1\rangle \;=\; \frac{1}{\sqrt{15}}\left[4\sqrt{3}\rho^{21}_{11} + 4\rho^{21}_{00} + 2\sqrt{5}\rho^{10}_{00}\right] \;, \qquad (4a)$$

$$\langle P_3\rangle \;=\; \frac{1}{7\sqrt{5}}\left[-12\rho^{21}_{11} + 6\sqrt{3}\rho^{21}_{00}\right] \;. \qquad (4b)$$

In particular, $\langle P_1\rangle$ is sensitive to P-wave interference with S and D-waves, whereas $\langle P_3\rangle$ is sensitive to only P-wave interference with a D-wave.

The relevant factorization theorem [4] has been proved only for longitudinal virtual photons γ^*_L in leading twist. Contributions from transverse photons γ^*_T and other higher-twist effects are suppressed by powers of $1/Q$. Therefore, the longitudinal terms ρ^{21}_{00} and ρ^{10}_{00} in Eqs. 4a and 4b are expected to be dominant in the $m_{\pi\pi}$ region far from the f_2 meson, where the higher-twist term ρ^{21}_{11} can be neglected. On the other hand, in the region of the f_2 resonance the possible ρ^{21}_{11} contribution can be eliminated by taking a combination of $\langle P_1\rangle$ and $\langle P_3\rangle$ that projects out the longitudinal terms:

$$\langle P_1 + \frac{7}{3}P_3\rangle \;=\; 2\sqrt{\frac{5}{3}}\rho^{21}_{00} + \frac{2}{\sqrt{3}}\rho^{10}_{00} \;. \qquad (5)$$

Assuming s-channel helicity conservation, such that the 0-helicity photon γ^*_L produces a $\pi^+\pi^-$ pair with 0-helicity, only ρ_{00} states are populated by γ^*_L. In this case, the combination $\langle P_1 + \frac{7}{3}P_3\rangle$ would be sensitive to longitudinal photons only. In the f_2 region, far from the ρ^0 and f_0 resonances, the term ρ^{10}_{00} is expected to vary very slowly with $m_{\pi\pi}$, making no contribution to any structure appearing in this combination.

In the $m_{\pi\pi}$ region of the f_2 meson, another combination eliminates the contribution of longitudinal tensor pairs:

$$\langle P_1 - \frac{14}{9}P_3\rangle \;=\; \frac{4\sqrt{5}}{3}\rho^{21}_{11} + \frac{2}{\sqrt{3}}\rho^{10}_{00} \;. \qquad (6)$$

Hence, the transverse higher-twist ρ^{21}_{11} and longitudinal leading-twist ρ^{21}_{00} contributions to the Legendre moments in the f_2 domain can be disentangled by comparing the combinations given above.

The data were collected with the HERMES spectrometer [13] during the running period 1996-2000. The

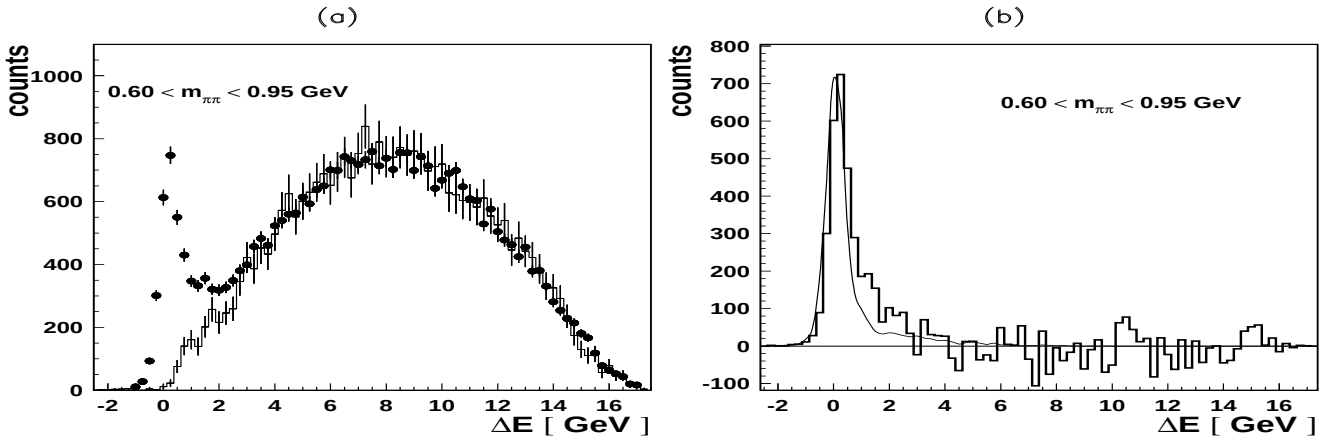

FIG. 2: Panel (a): Distribution of $\pi^+\pi^-$ events versus ΔE for hydrogen with $0.60 < m_{\pi\pi} < 0.95$ GeV. The data are represented by the solid circles, while the simulated (SIDIS) background is represented by the histogram. The Monte Carlo results are normalized to the data using the region of the spectrum above $\Delta E > 2$ GeV. Panel (b): Yield of the exclusive events as obtained by subtracting the normalized Monte Carlo events from the data. The result (thin line) of an arbitrarily normalized Monte Carlo simulation using the diffractive ρ^0 DIPSI generator is superimposed on the exclusive distribution.

27.6 GeV HERA positron beam at DESY was scattered off hydrogen and deuterium targets. Events were selected with exactly one positron track and two oppositely charged hadron tracks with momentum > 1 GeV, requiring that no additional neutral clusters occur in the calorimeter. Positrons were distinguished from hadrons with an average efficiency of 98%, and a hadron contamination below 1%, over the whole kinematic range. In order to ensure a hard scattering process, the constraints $Q^2 > 1$ GeV^2 and $W > 2$ GeV were imposed, where W is the invariant mass of the virtual photon-nucleon system.

When studying the $m_{\pi\pi}$-dependence of the Legendre moments, the requirement $x > 0.1$ was imposed to suppress the contribution from gluon-exchange relative to that from $q\bar{q}$ exchange [6]. However, when analyzing the x-dependence of the Legendre moments, the whole x-range accessible to HERMES was used.

Since the recoiling target nucleon is not detected in the present HERMES apparatus, exclusive events were selected by restricting the quantity $\Delta E = \frac{M_X^2 - M_{targ}^2}{2M_{targ}}$, in which M_X is the missing mass, and M_{targ} is the nucleon target mass. A ΔE distribution peaked at zero is a clear signature of exclusive production, while larger ΔE values indicate non-exclusive events. For scattering off nuclei, one can have either incoherent scattering from individual nucleons inside the target ($M_{targ} \approx M_N$) or coherent scattering from the entire nucleus A ($M_{targ} \approx M_A$). For scattering off deuterium, incoherent scattering is found to dominate for HERMES kinematics [14]; therefore M_{targ} was chosen to be the proton mass throughout the entire analysis. All detected hadrons have been treated as pions.

In the ΔE spectrum, the resolution due to instrumental effects ranges between 0.260 and 0.380 GeV, depending on the data production year. Thus, even at low ΔE the sample is contaminated by non-exclusive processes. This background yield was assumed to be semi-inclusive deep inelastic scattering (SIDIS) events and was evaluated by first calculating the ΔE distribution of SIDIS events with a Lepto Monte Carlo simulation [15, 16], and then normalizing it to the data in the range $\Delta E > 2$ GeV. The effect of varying this normalization region was treated as a systematic uncertainty contribution. Fig. 2 shows the normalized Monte Carlo distribution in ΔE compared to the data, and their difference. The simulated background shape is in agreement with the data at large ΔE, while at small ΔE the data show a surplus due to the presence of the exclusive process not included in that Monte Carlo simulation. Comparison of the exclusive peak in the data with the result of a Monte Carlo simulation using the diffractive ρ^0 DIPSI generator [17] reveals an excess at $\Delta E \approx 1.5$ GeV. This excess can be explained by the combined contributions of ρ^0 production via single and double-dissociation of the proton as described in Ref. [18], and of radiative corrections [19], which all three are not simulated by the DIPSI Monte Carlo.

In order to evaluate the background contribution to the exclusive signal, the experimental and the normalized Monte Carlo yields were separately integrated up to a limiting ΔE value ΔE_{cut}, resulting in N_{tot} and N_{MC} respectively. The value of ΔE_{cut} was optimized by requiring the ratio of the exclusive signal $N_{Sg} = N_{tot} - N_{MC}$ over the background (N_{Sg}/N_{Bg}) to be large, and the relative statistical uncertainty $\Delta N_{Sg}/N_{Sg}$ to be small. The optimized ΔE_{cut} value for both targets is 0.625 GeV. Be-

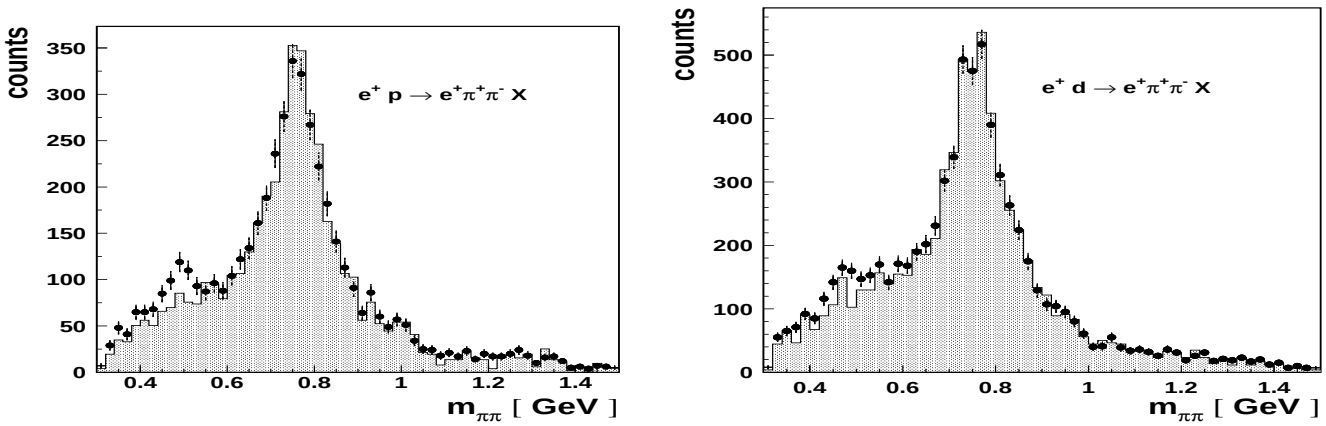

FIG. 3: Invariant mass spectrum for hydrogen (left) and deuterium (right) for $\Delta E < 0.625$ GeV (solid points) and $\Delta E < 0.125$ GeV (shaded area). For both spectra, the requirement $x > 0.1$ has been applied. For both targets, the $m_{\pi\pi}$-spectrum for $\Delta E < 0.125$ GeV is normalized and superimposed (shaded area) to show the suppression of the $\omega \to \pi^+\pi^-\pi^0$ contamination described in the text.

low the chosen ΔE_{cut} value, the SIDIS contamination is found to range between 2% and 65% of the total events, depending on $m_{\pi\pi}$ and x. In particular, this contamination is small at $m_{\pi\pi}$ values around m_{ρ^0}, and increases at smaller and larger invariant mass values.

The SIDIS model does not account for contamination from other processes. In order to suppress the $\omega \to \pi^+\pi^-\pi^0$ decay at low $m_{\pi\pi}$, as explained below, a more severe ΔE_{cut} was applied than the value optimized for the SIDIS background. The final ΔE_{cut} values used in this analysis for both targets are 0.125 GeV for $m_{\pi\pi} \leq 0.60$ GeV, and 0.625 GeV for $0.60 < m_{\pi\pi} \leq 1.40$ GeV.

The limited ΔE resolution does not allow for the complete suppression of single and double-dissociation processes. An example is the process in which the nucleon is left in a Δ resonance state that decays with an unobserved pion. The contamination from single and double-dissociation was estimated by shifting the value of ΔE_{cut} by 0.5 GeV, from a low value of 0.125 GeV where this contamination is negligible, to a relatively large value, 0.625 GeV, where this background is possibly substantial. This effect was included in the systematic uncertainty.

The contamination from target excitations such as $e^+p \to e^+\pi\Delta \to e^+p\pi^+\pi^-$, which have been found to contaminate the process $e^+p \to e^+p\pi^+\pi^-$ at lower energy and W values [20], in the HERMES kinematics were found to be negligible in a Dalitz-plot analysis [21].

The contamination of exclusive K^+K^- pairs from $\phi(1020)$ meson decay, which appears in the event yield at $m_{\pi\pi} \approx 0.35$ GeV, is entirely eliminated by applying the additional cut $m_{KK} > 1.06$ GeV. Here m_{KK} is the invariant mass of the two hadrons when they are treated as kaons. Similarly, the contamination of $\phi \to K_S K_L$, with K_S detected through its decay in $\pi^+\pi^-$, by using a Monte Carlo DIPSI simulation was found to be entirely absent within the chosen ΔE_{cut} values. The channel $\omega \to \pi^+\pi^-$ and exclusive non-resonant K^+K^- [1] production were estimated to contaminate the signal by less than 0.3% and 1.5%, respectively, and were neglected. The decays $\phi \to \pi^+\pi^-\pi^0$ [2], with the π^0 outside the acceptance, gives a contamination of less than 1%. A contamination of about 18% from the decay $\omega \to \pi^+\pi^-\pi^0$, with only the charged tracks detected, yields a reconstructed $m_{\pi\pi}$ distribution centered at 0.45 GeV with a Gaussian width of approximately 0.075 GeV [22]. This contribution to the yield was suppressed by imposing $\Delta E < 0.125$ GeV in the region $m_{\pi\pi} \leq 0.6$ GeV. The effect of the remaining contamination was taken into account in the systematic uncertainty of the relevant bins. All the above estimations of these additional background components are small compared to the background predicted by the SIDIS model.

After applying all event selection requirements, 4.8×10^3 (7.2×10^3) $\pi^+\pi^-$ events remained for the $m_{\pi\pi}$-dependence analysis with $x > 0.1$, and 11.0×10^3 (13.3×10^3) events for the x-dependence analysis for hydrogen (deuterium). The invariant mass spectra for hydrogen and deuterium with $\Delta E < 0.625$ GeV, $x > 0.1$, and $m_{KK} > 1.06$ GeV are shown in Fig. 3.

In each of the analyzed bins, $\langle P_n \rangle_{data}$ was evaluated within the chosen exclusive ΔE region, with no back-

[1] This contamination has been estimated by comparing results from the data and the Monte Carlo simulation of SIDIS events.
[2] Including the resonant channel $\phi \to \rho\pi \to \pi^+\pi^-\pi^0$.

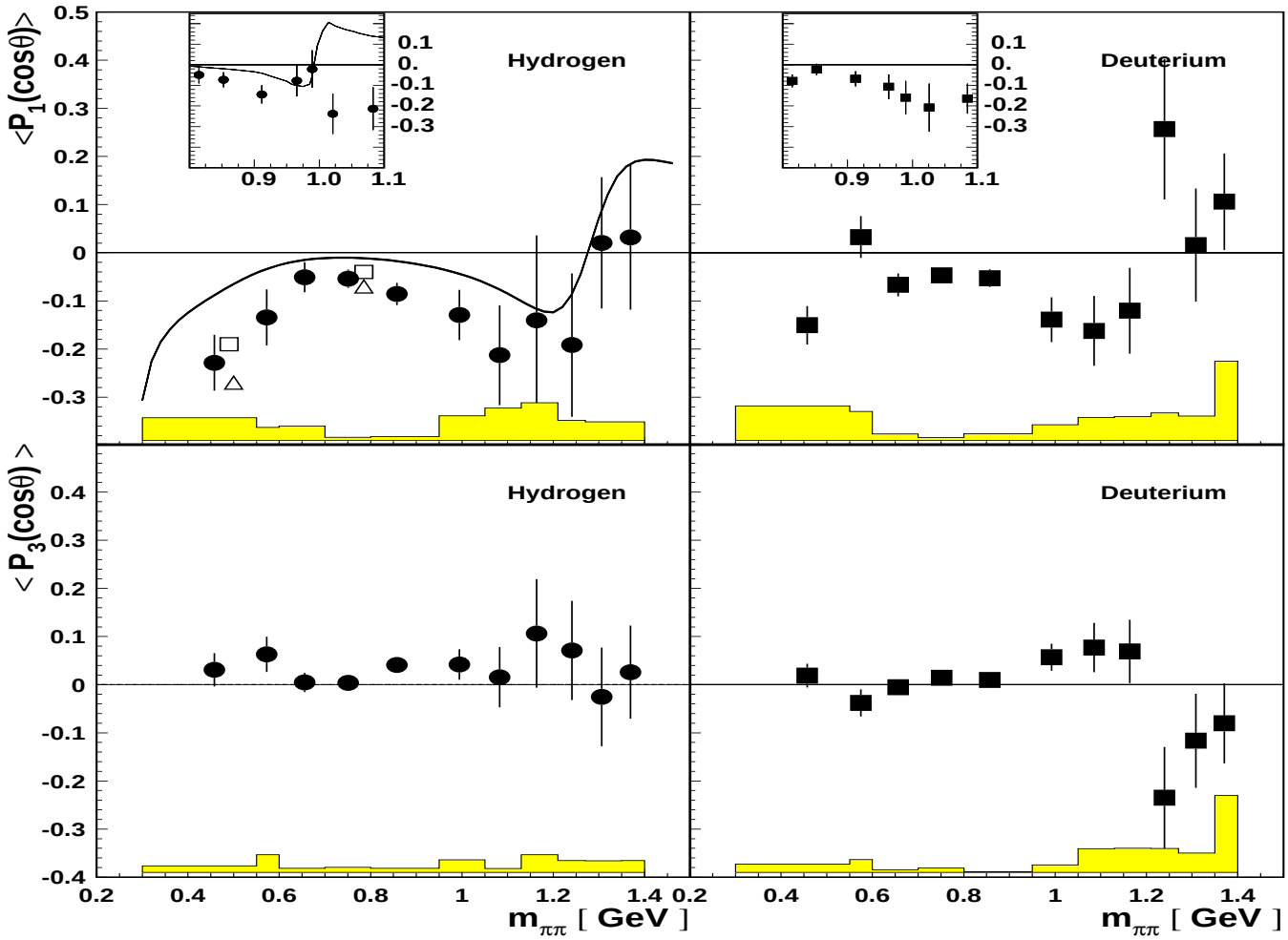

FIG. 4: The $m_{\pi\pi}$-dependence of the Legendre moments $\langle P_1\rangle$ (upper panels) and $\langle P_3\rangle$ (lower panels) for hydrogen (left panels) and deuterium (right panels), for $x > 0.1$. The region $0.8 < m_{\pi\pi} < 1.1$ GeV is presented with finer bins to better investigate possible contributions from the narrow $f_0(980)$ resonance, as shown in the insert. In the upper panels, leading twist predictions for the hydrogen target including the two-gluon exchange mechanism contribution, LSPG [6, 7] (solid curve) at $x = 0.16$ are shown. A calculation without the gluon exchange contribution is shown for limited $m_{\pi\pi}$ values, LPPSG [8] (open squares at $x = 0.1$, open triangles at $x = 0.2$). In these calculations, the contribution from f_0 meson decay was not considered. Instead, the inset panel for the hydrogen target shows the prediction from [25], which includes the f_0 meson contribution. All experimental data have $\langle x\rangle = 0.16$, $\langle Q^2\rangle = 3.2$ (3.3) GeV^2, and $\langle -t\rangle = 0.43$ (0.29) GeV^2 for hydrogen (deuterium). The systematic uncertainty is represented by the error band.

ground subtraction. The values of $\langle P_n\rangle_{SIDIS}$ for the background events were extracted from the data for $\Delta E > 2$ GeV, where SIDIS events dominate. These values were found to be consistent when evaluated in three different ΔE bins: $2 < \Delta E < 4$ GeV, $4 < \Delta E < 6$ GeV, and $\Delta E > 6$ GeV. The moments were corrected for SIDIS background using

$$\langle P_n\rangle_{\rm exclusive} = \frac{1+r}{r}\langle P_n\rangle_{\rm data} - \frac{1}{r}\langle P_n\rangle_{\rm SIDIS}\ , \qquad (7)$$

in which r is the ratio of integrated exclusive data to background Monte Carlo events for $\Delta E < \Delta E_{cut}$ in the analyzed bin.

A Monte Carlo generator based on the GPD framework for the hard $\pi^+\pi^-$ exclusive process does not exist. Therefore the DIPSI generator was used to evaluate the effects of geometric acceptance and instrumental smearing on the Legendre moments, which were both found to be negligible [21]. This Monte Carlo simulation is in good agreement with the kinematic distributions of exclusive ρ^0 mesons observed at HERMES.

The analyzed moments might be sensitive to radiative corrections that affect the $\cos\theta$ angular distribution. For ρ^0 decay, which dominates in the cross section for exclusive $\pi^+\pi^-$ production, the angular distribution depends

linearly only on the vector spin density matrix element r^{04}_{00}. In previous work [23] the relative correction of r^{04}_{00} for radiative corrections has been evaluated, and found to be less than 0.3% at $\langle Q^2\rangle \approx 3$ GeV^2 in the kinematics of the H1 and ZEUS experiments. At larger x, where the HERMES analysis is performed, they are even smaller. As a result of these considerations, radiative corrections effects have been neglected in this analysis.

The $m_{\pi\pi}$-dependence of $\langle P_1\rangle$ and $\langle P_3\rangle$ for exclusive $\pi^+\pi^-$ production off hydrogen and deuterium is presented in Fig. 4, for $x > 0.1$. The average values of Q^2, $-t$, and x for both targets in this domain are reported in Tab. I. For $m_{\pi\pi} < 1$ GeV, the moments are similar for the two targets. In each panel for $\langle P_1\rangle$, the region $0.8 < m_{\pi\pi} < 1.1$ GeV is shown as an insert with finer binning to better investigate possible contributions from the narrow $f_0(980)$ resonance.

The values for $\langle P_1\rangle$ differ significantly from zero, and depend strongly on $m_{\pi\pi}$. At small invariant mass, i.e. close to the threshold $2m_\pi$, this non-zero moment is interpreted as originating from the interference between the lower tail of the isovector $\rho^0(770)$ (P-wave) with the S-wave non-resonant $\pi^+\pi^-$ amplitude. At $m_{\pi\pi}$ values around m_{ρ^0}, the absolute value of this quantity shows a minimum, which is explained in terms of the overwhelming dominance of ρ^0 vector meson production in the denominator of the moment. The increase of the size of $\langle P_1\rangle$ at larger invariant mass is due to the interference of the upper tail of the ρ^0 with the non-resonant $\pi^+\pi^-$ S-wave production. At $m_{\pi\pi} \approx 1$ GeV, the observed oscillation in hydrogen $\langle P_1\rangle$ suggests an interference between the ρ^0 tail and the S-wave $\pi^+\pi^-$ production from the narrow $f_0(980)$ resonance. Moreover, in the $f_2(1270)$ meson region, the data suggest a sign change caused by the interference between the ρ^0 upper tail and the f_2 (D-wave).

The Legendre moment $\langle P_3\rangle$ is sensitive only to the interference of P-wave and D-wave states in $\pi^+\pi^-$ production. Consistent with the expectation that no resonance decay into $\pi^+\pi^-$ pairs in D-wave states occurs for $m_{\pi\pi} \leq 1$ GeV, no interference is observed in this invariant mass region. The $\langle P_3\rangle$ moment for deuterium increases in magnitude in the $f_2(1270)$ meson region. A sign change is also prominently visible, reflecting the interference of the P-wave and D-wave resonant $\pi^+\pi^-$ channels. On the other hand, no such signature is evident in the hydrogen data.

In Fig. 4 the $m_{\pi\pi}$-dependence of $\langle P_1\rangle$ for hydrogen is compared with theoretical calculations based on the GPD framework, with [6, 7] (solid curve) and without [8] (open points) the inclusion of the two-gluon exchange mechanism. A possible contribution from the f_0 meson was not considered in the calculations. The calculations include only the longitudinal component σ_L of the $\pi^+\pi^-$ cross section, while in this analysis no separation between the σ_L and σ_T contributions could be made. The σ_T contribution to the total cross section for ρ^0 production is

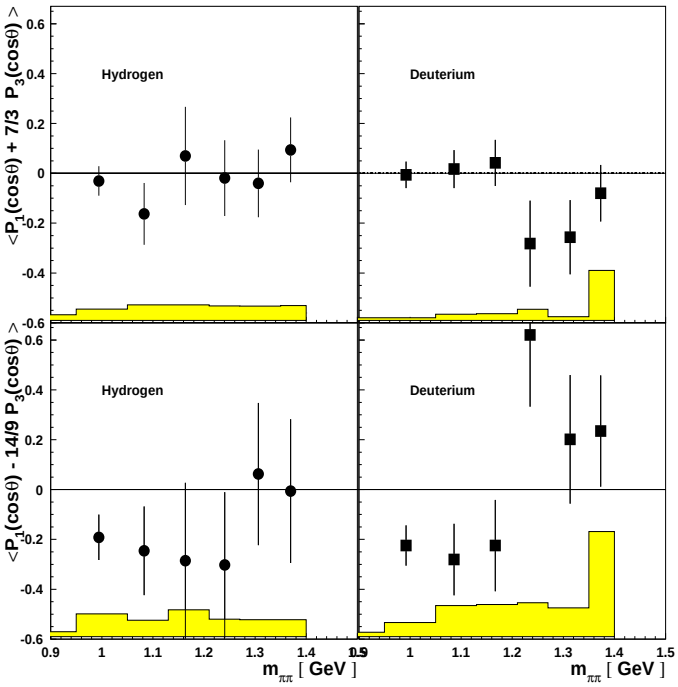

FIG. 5: The $m_{\pi\pi}$-dependence of $\langle P_1 + 7/3 \cdot P_3\rangle$ (upper panels) and $\langle P_1 - 14/9 \cdot P_3\rangle$ (lower panels) for hydrogen (left panels) and deuterium (right panels). The data have $\langle x\rangle = 0.16$, $\langle Q^2\rangle = 3.2$ (3.3) GeV^2, and $\langle -t\rangle = 0.43$ (0.29) GeV^2 for hydrogen (deuterium). The systematic uncertainty is represented by the error band.

estimated to be approximately 60% [18]. The reasonable agreement of the leading twist predictions for the $m_{\pi\pi}$-dependence of the $\langle P_1\rangle$ data may tentatively be understood as arising from the cancellation of higher twist effects in this moment [24].

To date, the f_0 contribution is taken into account only by Ref. [25], where the discussion is restricted to diffractive physics at center-of-mass energies larger than 100 GeV. Nevertheless, to demonstrate the possible effect of this resonance, the comparison with those predictions for $\langle P_1\rangle$ on hydrogen is shown in the panel insert of Fig. 4.

In order to study the contribution of the f_2 resonance to the Legendre moments in more detail, the $m_{\pi\pi}$-dependence of the purely longitudinal combination $\langle P_1 + \frac{7}{3} \cdot P_3\rangle$ is presented in Fig. 5 for both hydrogen and deuterium. For comparison, this figure also shows the combination $\langle P_1 - \frac{14}{9} \cdot P_3\rangle$ which is believed to be dominated by the higher-twist transverse contribution to the excitation of the f_2 resonance. The comparison between these two distributions suggests that the higher-twist transverse contribution to the Legendre moments in the $f_2(1270)$ region is possibly as large as the longitudinal leading-twist production.

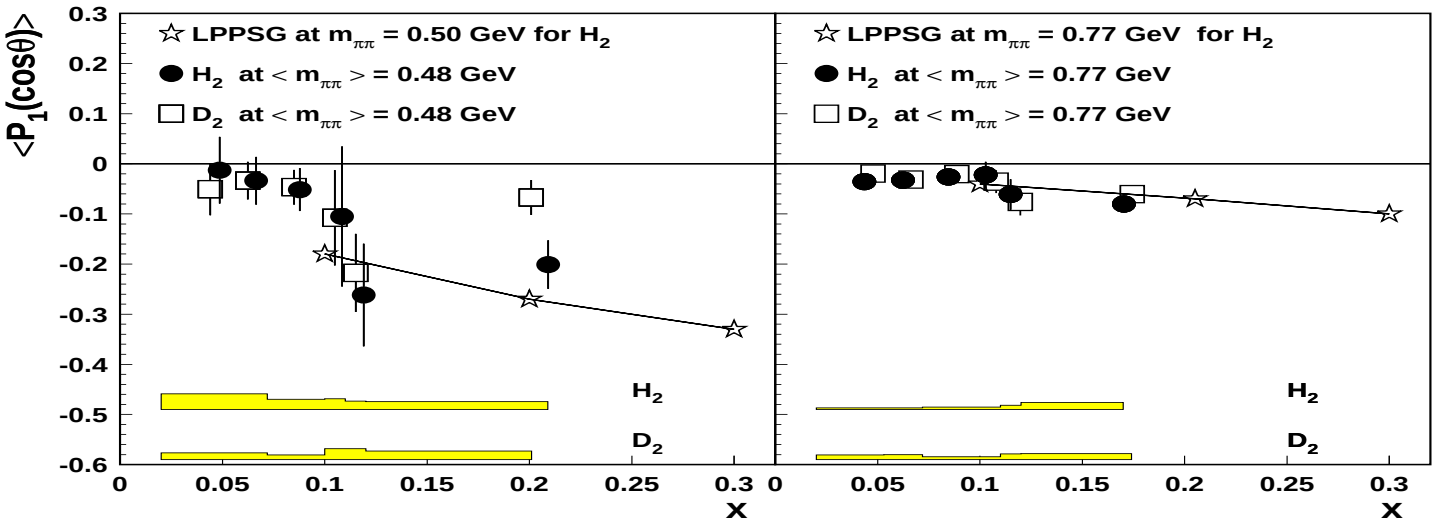

FIG. 6: The x-dependence of the Legendre moments $\langle P_1 \rangle$ for both targets separately, in the regions $0.30 < m_{\pi\pi} < 0.60$ GeV (left panel) and $0.60 < m_{\pi\pi} < 0.95$ GeV (right panel). The systematic uncertainty is given by the error band. Theoretical predictions (stars) from LPPSG [8] for hydrogen, which neglect two-gluon exchange mechanism, are compared with the data.

The x-dependence of $\langle P_1 \rangle$ is shown in Fig. 6 for both targets in two regions of $m_{\pi\pi}$: $0.30 < m_{\pi\pi} < 0.60$ GeV and $0.60 < m_{\pi\pi} < 0.95$ GeV. The statistical precision at larger values of $m_{\pi\pi}$ is insufficient for such a presentation. The average values of Q^2, $-t$, and x for both targets in these $m_{\pi\pi}$ regions are reported in Table I. In both invariant mass regions and for both targets, $\langle P_1 \rangle$ is non-zero, which we interpret as originating from the interference of resonant ρ^0 P-wave with non-resonant S-wave $\pi^+\pi^-$ production. The moment increases in magnitude with x, suggesting that the exchange of flavour non-singlet quark combinations ($C = -1$) becomes competitive with the dominant singlet exchange ($C = +1$). Predictions with only the quark exchange mechanism in the GPD framework [8] are compared with the data, and are found to be in fair agreement with them.

In summary, the Legendre moments $\langle P_1(\cos\theta) \rangle$ and $\langle P_3(\cos\theta) \rangle$ for exclusive electroproduction of $\pi^+\pi^-$ pairs have been measured for the first time for hydrogen and deuterium targets. The data show signatures of the interference between the dominant isospin state $I = 1$ (P-wave) and $I = 0$ (S, D-wave) of these pion pairs. The interference of the ρ^0 amplitude with the non-resonant S-wave and resonant D-wave states appears to be larger than the interference with the resonant f_0 S-wave. In the f_2 region, the combinations $\langle P_1 + 7/3 \cdot P_3 \rangle$ and $\langle P_1 - 14/9 \cdot P_3 \rangle$ are sensitive to the longitudinal and the transverse states of a D-wave $\pi^+\pi^-$ pair, respectively. Comparison of these combinations suggests that, at $\langle Q^2 \rangle = 3$ GeV^2, the higher-twist transverse contribution to the Legendre moments in the f_2 domain can be as large as the leading-twist longitudinal contribution.

These results constrain models for Generalized Parton Distributions, and may allow, by comparing the data with a larger statistical significance with the more accurate next-to-leading order predictions with and without the inclusion of the two-gluon mechanism, the separation of the contributions of two-gluon and $q\bar{q}$ exchange mechanisms, which are connected to the quark and gluon content of the nucleon.

We are grateful for inspiring and helpful discussions with M. Diehl, B. Lehmann-Dronke, B. Pire and M. V. Polyakov. We gratefully acknowledge the DESY management for its support, the staff at DESY, and the collaborating institutions for their significant effort. This work was supported by the FWO-Flanders, Belgium; the Natural Sciences and Engineering Research Council of Canada; the ESOP, INTAS and TMR network contributions from the European Union; the German Bundesministerium für Bildung und Forschung; the Italian Instituto Nazionale di Fisica Nucleare (INFN); Monbusho International Scientific Research Program, JSPS and Toray Science Foundation of Japan; the Dutch Foundation for Fundamenteel Onderzoek der Materie (FOM); the U.K. Particle Physics and Astronomy Research Council; and the U.S. Department of Energy and National Science Foundation.

[1] D. Müller et al., Fortsch. Phys. **42** (1994) 101.

$m_{\pi\pi}$-dependence analysis			
Target	$\langle Q^2 \rangle$ [GeV^2]	$\langle -t \rangle$ [GeV^2]	$\langle x \rangle$
H	3.2	0.43	0.16
D	3.3	0.29	0.16

x-dependence analysis				
	$\langle m_{\pi\pi} \rangle = 0.48$ **[GeV]**		$\langle m_{\pi\pi} \rangle = 0.77$ **[GeV]**	
Target	$\langle Q^2 \rangle$ [GeV^2]	$\langle -t \rangle$ [GeV^2]	$\langle Q^2 \rangle$ [GeV^2]	$\langle -t \rangle$ [GeV^2]
H	2.3	0.42	2.1	0.27
D	2.3	0.39	2.1	0.22

TABLE I: Average values for $\langle Q^2 \rangle$, $\langle -t \rangle$, and $\langle x \rangle$ measured in the $m_{\pi\pi}$- (upper table) and x- (bottom table) dependence of Legendre moments for hydrogen and deuterium targets.

[2] A. V. Radyushkin, Phys. Rev. D **56** (1997) 5524.
[3] X. Ji, J. Phys. G **24** (1998) 1181.
[4] J. Collins, L. Frankfurt and M. Strikman, Phys. Rev. D **56** (1997) 2982.
[5] A. Freund, Phys. Rev. D **61** (2000) 074010.
[6] B. Lehmann-Dronke et al., Phys. Rev. D **63** (2001) 114001.
[7] B. Lehmann-Dronke, Private Communication.
[8] B. Lehmann-Dronke et al., Phys. Lett. **B475** (2000) 147.
[9] M. Diehl, Private Communication.
[10] HERMES Coll., A. Airapetian et al., Eur. Phys. Jour. **C 17** (2000) 389.
[11] M. Diehl, Phys. Rept. **388** (2003) 41.
[12] R.L.Sekulin, Nucl. Phys. **B56** (1973) 227.
[13] HERMES Coll., K. Ackerstaff et al., Nucl. Inst. and Methods **A 417** (1998) 230.
[14] HERMES Coll., K. Ackerstaff et al., Phys. Rev. Lett. 82 (1999) 3025-3029.
[15] G. Ingelman, A. Edin and J. Rathsman, Comp. Phys. Comm. **101** (1997) 108.
[16] B. Andersson et al., Phys. Rep. **97** (1983) 31.
[17] M. Arneodo, L. Lamberti and M. Ryskin, Phys. Comp. Comm. **100** (1997) 195.
[18] HERMES Coll., A. Airapetian et al., Eur. Phys. Jour. **C 18** (2000) 303.
[19] E.-C. Aschenauer, P. Liebing, and T. Sjöstrand, (in preparation).
[20] CLAS Coll., M. Ripani et al., Phys. Rev. Lett. 91 (2003) 022002.
[21] R. Fabbri, PhD Thesis, University of Ferrara 2003, HERMES-03-036.
[22] M. Tytgat, PhD Thesis, University of Gent 2001, DESY-THESIS-2001-018.
[23] I. Akushevich and P. Kuzhir, Phys. Lett. **B474** (2000) 411.
[24] M. Garçon, Eur. Phys. Jour. **A 18** (2003) 389.
[25] Ph. Hägler et al., Eur. Phys. Jour. **C 26** (2002) 261.